Journal of Colloid and Interface Science 687 (2025) 582–588

Contents lists available at ScienceDirect

Journal of Colloid And Interface Science

journal homepage: www.elsevier.com/locate/jcis

Regular Article

Selective crystallization of pyrazinamide polymorphs in supramolecular gels: Synergistic selectivity by mimetic gelator and solvent

Qi Zhang [a,b], Yizhen Yan [c], Yisheng Xu [a], Xiangyang Zhang [a,*], Jonathan W. Steed [b,*]

[a] State Key Laboratory of Chemical Engineering, East China University of Science and Technology, Shanghai 200237, China
[b] Department of Chemistry, Durham University, Durham DH1 3LE, UK
[c] Department of Engineering and Design, School of Engineering and Information, University of Sussex, Brighton BN1 9RH, UK

GRAPHICAL ABSTRACT

A pyrazinamide-mimetic gelator templates metastable Forms β and δ of pyrazinamide by gel phase crystallization. This approach is the only known way to access the pure Form β at room temperature.

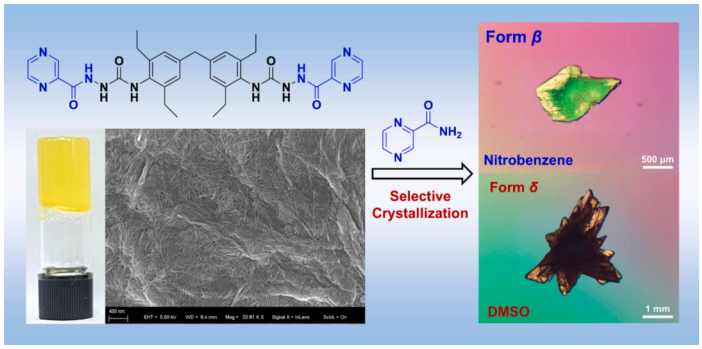

ARTICLE INFO

Keywords:
Gel phase crystallization
Pharmaceutical polymorph
Pyrazinamide
Mimetic gelator
Solvent effect

ABSTRACT

A mimetic gelator designed to incorporate the chemical structure of pyrazinamide (PZA), a highly polymorphic drug, has been synthesized. Metastable Forms β and δ of PZA were obtained from supramolecular gel phase crystallization in nitrobenzene and DMSO, respectively, using a bis(urea) gelator designed to mimic the structure of PZA. This is the only known way to access the pure Form β at room temperature. In contrast, concomitant crystallization of a mixture of metastable polymorphs and the most thermodynamically stable form were obtained from solution crystallization. By analyzing the intermolecular interactions of PZA in the mimetic gel phase crystallization, it is proposed that the mimetic gelator and solvent can influence the nucleation behavior by close interaction with the carbonyl group to select PZA Forms β and δ.

1. Introduction

Controlling pharmaceutical polymorphism is crucial in drug development, as different polymorphs could cause variations in therapeutic efficacy and manufacturing processes [1,2]. However, the selective crystallization of desired polymorphs, particularly metastable forms

* Corresponding authors.
E-mail addresses: zxydcom@ecust.edu.cn (X. Zhang), jon.steed@durham.ac.uk (J.W. Steed).

https://doi.org/10.1016/j.jcis.2025.02.093
Received 19 December 2024; Received in revised form 10 February 2025; Accepted 14 February 2025
Available online 16 February 2025
0021-9797/© 2025 The Authors. Published by Elsevier Inc. This is an open access article under the CC BY license (http://creativecommons.org/licenses/by/4.0/).

that may offer enhanced solubility or bioavailability, remains a significant challenge [3,4]. The use of gel phase crystallization to control polymorphism in pharmaceutical compounds has emerged as a powerful tool [5–7]. Compared to conventional solution crystallization, gel phase crystallization offers several advantages, including a micro-confined environment that potentially limits molecular diffusion and convection and an active surface that can influence crystal nucleation and growth [8,9]. By tailoring a supramolecular gel matrix, researchers have observed the control over polymorph formation or unique crystallization outcomes that are difficult to achieve in solution [10,11].

The development of drug mimetic gels represents a novel approach for gel phase crystallization [5,12–14]. By incorporating moieties from the drug structure into the gelator, the mimetic gel can act as a specific surface for heterogeneous nucleation and potentially provide a template to encourage the epitaxial overgrowth of specific packing structure of drug crystals and/or induce the bias in conformational distribution of drug molecules during nucleation, resulting in the formation of metastable or difficult-to-nucleate solid forms [15–18]. At the end of crystallization, gelation can be turned off by the addition of anions, allowing pure crystals to be retrieved by filtration [11,19]. A series of mimetic gelators have been developed for the crystallization of various drugs, including ROY-mimetic gelators with a similar torsion angle as the metastable Form R [15], imide group-containing mimetic gelators for preventing concomitant crystallization of thalidomide and barbital [18], cisplatin-mimetic gelators giving rise to a novel solvate [20], and mexiletine hydrochloride-mimetic gelators that induce different metastable salt polymorphs [21]. However, the interaction mode of mimetic gels with drug molecules is not clear, and the role of solvent in the gel still requires further exploration.

Pyrazinamide (PZA), a widely used antituberculosis drug [22,23], is a classic example of packing polymorphism of pharmaceutical compound [24]. Despite its simple molecular structure, PZA exhibits complex polymorphism, including thermodynamically stable under ambient conditions Form α and metastable Forms β, δ, and γ [24–28]. The stability, solubility and structure properties of different PZA polymorphs have been extensively studied [24,29–32]. In solution crystallization, PZA tends to form a mixture of metastable polymorphs by concomitant polymorphism [33]. Even heterogeneous crystallizations containing tailored additives [34,35], polymers [36], hydrogels [37] and functional group templates [38] have failed to give rise to the pure Form β.

In this study, we have designed a PZA-mimetic gelator and explored PZA polymorphism in mimetic supramolecular gel phase crystallization. PZA Forms β and δ were selectively obtained in nitrobenzene and DMSO gels, which was the first time pure Form β has been obtained. By comparing polymorph outcomes with solution and non-mimetic gel phase crystallization, the advantage of mimetic gel phase crystallization in obtaining pure metastable polymorphs of PZA is illustrated. The role of mimetic gelator and solvent in the selective crystallization of PZA is further explained by gel surface crystallization and gel phase crystallization in mixed solvents. Finally, we explore how the mimetic gel influences the intermolecular interactions of PZA during nucleation.

2. Experimental

2.1. Materials

Pyrazinoic acid hydrazide and pyrazinamide were purchased from Fluorochem (UK). 4,4′-methylenebis (2,6-diethylphenyl isocyanate), propylamine, triethylamine and tetrabutylammonium acetate were purchased from Sigma Aldrich (UK). All organic solvents were from Fisher Scientific (UK). All chemicals and reagents are of analytical purity.

2.2. Synthesis

2.2.1. Mimetic gelator

Pyrazinoic acid hydrazide (276.2 mg, 2.0 mmol) was added in chloroform (40 mL) with a slight excess of triethylamine and heated to obtain a clarified solution. 4,4′-methylenebis(2,6-diethylphenyl isocyanate) (362.5 mg, 1.0 mmol) was dissolved in chloroform (10 mL) and added dropwise to the pyrazinoic acid hydrazide solution. The mixture was heated under reflux at 70 °C for 12 h, cooled to room temperature, and filtered. The precipitate was then washed twice with chloroform and diethyl ether, and dried. The solid was ground as a fine yellow powder (568.1 mg, 0.89 mmol, 89 %).

^{1}H NMR (400 MHz, DMSO-d_6) δ = 10.53 (s, 2H, PzCONH), 9.18 (d, J = 1.5, 2H, PzH), 8.87 (d, J = 2.4, 2H, PzH), 8.74 (dd, J = 2.5, 1.5, 2H, PzH), 8.20 (s, 2H, PzCONHNH), 7.85 (s, 2H, PhNH), 6.92 (s, 4H, PhH$_2$), 3.83 (s, 2H, PhCH$_2$Ph), 2.53 (t, J = 7.4, 8H, PhCH$_2$), 1.08 (t, J = 7.5, 12H, PhCH$_2$CH$_3$). Elemental analysis for $C_{33}H_{38}N_{10}O_4$: Calc. (%): C 62.05, H 6.00, N 21.93; Found (%): C 61.52, H 5.96, N 21.65.

2.2.2. Non-mimetic gelator

4,4′-methylenebis (2,6-diethylphenyl isocyanate) (543.7 mg, 1.5 mmol) was dissolved in 20 mL of tetrahydrofuran and propylamine (177.3 mg, 3.0 mmol) was added with stirring, rapidly appearing as a white gel. The reaction was stirred for 4 h at room temperature and filtered. The precipitate was then washed with dichloromethane and diethyl ether and dried. The solid was ground as a fine white powder (620.1 mg, 1.29 mmol, 86 %).

^{1}H NMR (400 MHz, DMSO-d_6) δ = 7.22 (s, 2H, CH$_2$NHCO), 6.93 (s, 4H, PhH$_2$), 5.93 (s, 2H, PhNH), 3.80 (s, 2H, PhCH$_2$Ph), 2.98 (q, J = 6.6, 4H, NHCH$_2$), 2.46 (t, J = 7.5, 8H, PhCH$_2$), 1.39 (h, J = 7.0, 4H, NHCH$_2$CH$_2$), 1.07 (t, J = 7.6, 12H, PhCH$_2$CH$_3$), 0.84 (t, J = 7.4, 6H, NHCH$_2$CH$_2$CH$_3$). Elemental analysis for $C_{29}H_{44}N_4O_2$: Calc. (%): C 72.46, H 9.23, N 11.66; Found (%): C 72.16, H 9.08, N 11.42.

2.3. Preparation of gel

A certain proportion of gelator and solvent (see Section 1 of the SI for details) was added in a glass vial and heated slowly with a heat gun until the gelator fully dissolved. The mixture was sonicated for about 10 s to promote gel formation and then left to cool slowly to room temperature. Gelation was confirmed by performing a “stable-to-inversion” test on the aggregated material in the vial.

2.4. Crystallization methods

2.4.1. Gel phase crystallization

A certain amount of PZA and gelator was added to the solvent (see Section 3 of the SI for details) and the PZA −containing gel was obtained according to the method of gel preparation. PZA was added in a supersaturated amount, resulting in crystals in the gel phase at room temperature within 30 min to 2 days. To collect the PZA crystals, tetrabutylammonium acetate was added to break down the gel structure and then the crystals were separated by filtration.

2.4.2. Solution crystallization

Under the same condition as gel phase crystallization, the solution containing supersaturated PZA was obtained by heating, crystallized at room temperature and filtered to obtain crystals. The solution with the addition of mimetic gelator followed the same method as solution crystallization, where the gelator was added to the solvent along with the PZA.

2.4.3. Gel surface crystallization

The saturated solution of PZA in nitrobenzene or DMSO at 60 °C was prepared and then added dropwise to the surface of nitrobenzene mimetic gel at room temperature, with standing to obtain PZA crystals

on the gel surface.

2.5. Characterization methods

2.5.1. Scanning electron microscopy (SEM)

SEM samples were prepared on silicon wafers, dried at room temperature, and sputter-coated with 2 nm of platinum. The images were obtained using an FEI Helios NanoLab DualBeam microscope in immersion mode, with beam settings of 1.5 kV and 0.17 nA.

2.5.2. Polarizing optical microscopy (POM)

The morphologies of PZA crystals were characterized by POM with OLYMPUS SZX12.

2.5.3. Powder X-ray diffraction (PXRD)

The polymorph of PZA crystals was identified by PXRD with Bruker D8 Advance. The sample was placed in a diffractometer with Cu Kα radiation, collecting the pattern in the range of 5–50° at a scanning rate of 10°/min.

2.5.4. Fourier transform infrared (FTIR)

FTIR spectrum was measured on a Perki Elmer Spectrum 100 instrument using direct compression method in the wavelength range of 4000–550 cm^{-1}.

2.6. Calculation methods

The standard PXRD patterns were obtained by simulating the PZA single crystal structures from the Cambridge Structure Data (CSD) using Mercury software, with refcodes PYRZIN [39], PYRZIN01 [40], PYRZIN02 [41], PYRZIN17 [33] for Forms α, β, δ and γ, respectively.

Hirshfeld surfaces of Forms β and δ were calculated using the Crystal Explorer software [42]. The 2D fingerprint plots derived from the Hirshfeld surface were analyzed to distinguish the different packing modes of PZA polymorphs.

3. Results and discussion

3.1. Preparation of mimetic gel

A pyrazinamide-mimetic gelator was synthesized in high yield by a nucleophilic addition reaction of pyrazinoic acid hydrazide with the corresponding terminal isocyanate-containing linker at a 2:1 ratio, as described in the experimental section. The compound contains two urea groups to form supramolecular gels primarily through intermolecular hydrogen bonding interaction and two functional groups similar to the structure of PZA, as shown in Fig. 1a. The supramolecular gel is readily prepared by simply heating and dissolving the gelator in a solvent and then sonicating at room temperature.

Gel screening was performed on the PYZ-mimetic gelator. Despite screening 40 candidate solvents, the gelator displayed solubility and gelation in only a few solvents (Table S1). Fig. 1b shows the four gels formed in nitrobenzene, N,*N*-dimethylformamide (DMF), N,*N*-dimethylacetamide (DMA) and dimethyl sulfoxide (DMSO) at the critical gel concentration (CGC) values of 1.6, 2.0, 2.5 and 5.6 % w/v, respectively. The morphology of the resulting xerogels were further characterized by SEM. Fig. 1c shows the entangled nanofibrillar structure of the gel that is highly cross-linked. The formation of entangled fibers demonstrates that the mimetic gelator can self-assemble multiple molecular chains to create cross-linked aggregates to further form the supramolecular gel network, possibly via a scrolling mechanism [43,44].

3.2. Gel phase crystallization of PZA

We tried to use the four prepared mimetic gels for gel phase crystallization of PZA. However, for the DMF and DMA gels, gelation ceased when PZA was added, and gels could not be obtained even when the gelator concentration was increased. This may be related to an inhibition of the inter-fiber interaction leading to the gel fiber formation by PZA molecules in these solvents, or inhibition of fiber formation by competitive hydrogen bonding [45]. The gelation of nitrobenzene and DMSO gels was not affected at the corresponding CGC values and these gels were therefore used for the subsequent PZA gel phase crystallization studies.

PZA crystals were obtained by dissolving the supersaturated PZA and mimetic gelator with heat and standing at room temperature for 30 min to 24 h in nitrobenzene and DMSO gel phases. The gel was then dissolved by addition of tetrabutylammonium acetate to obtain the isolated PZA crystals by filtration. Fig. 2a shows the millimeter-scale crystals with different morphologies obtained from the mimetic gels. The PZA crystals occur as white flakes from the nitrobenzene gel and as fused white plates from the DMSO gel. The polymorphs of the obtained PZA crystals were identified by PXRD, as shown in Fig. 2b. By comparison with the simulated PXRD patterns obtained from the known single crystal structures of PZA [33,39–41], the PZA crystals obtained from nitrobenzene gel were identified as Form β, and those obtained from DMSO gel as Form δ. Forms β and δ are both metastable polymorphs of PZA, and Form β especially is the most unstable and often appears in concomitant mixtures of polymorphs [24,33], leading to difficult preparation by conventional crystallization methods. The formation of pure

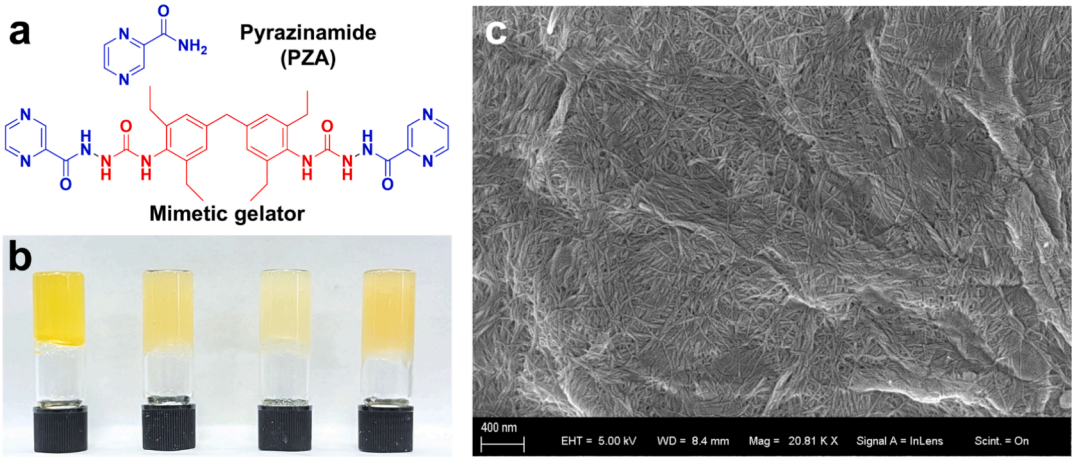

Fig. 1. (a) Chemical structure of pyrazinamide and mimetic gelator; (b) gels at CGC in (left to right) nitrobenzene, DMF, DMA and DMSO; (c) SEM image of the mimetic xerogel at 1.6 % w/v in nitrobenzene.

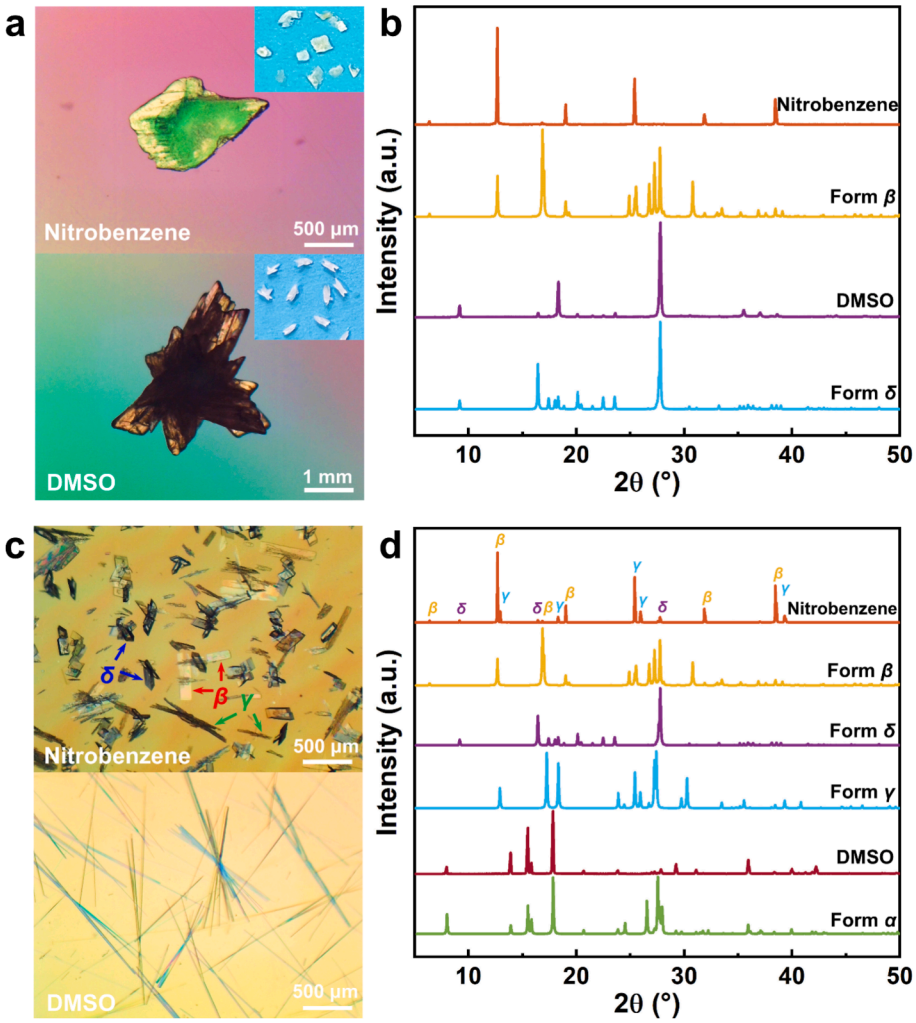

Fig. 2. (a–b) Crystal morphologies and PXRD patterns of PZA in nitrobenzene and DMSO gel phase crystallization; (c–d) crystal morphologies and PXRD patterns of PZA in nitrobenzene and DMSO solution crystallization.

Form β in the gel illustrates the significant advantage of the mimetic gel approach in obtaining the pure metastable polymorph. This is also the only known way to obtain the pure Form β at room temperature, which Form β has higher solubility and bioavailability and contributes to understanding the polymorphic transformation process. Besides, gel phase crystallizations with varying gelator concentration and PZA supersaturation were also performed, with no influence on the polymorphic outcome of the PZA (Table S2 for experimental details).

Solution crystallization with the same conditions as gel phase crystallization was carried out as a control (Table S3 for experimental details). PZA crystals obtained by solution crystallization in pure solvent had different crystal morphologies and polymorphism from the gel phase crystallization. Fig. 2c shows the mixed crystals of flakes, plates and rods obtained from nitrobenzene and the crystals of needles in DMSO by solution crystallization. PXRD data indicate that the PZA crystals obtained from nitrobenzene are mixed polymorphs of Forms β, δ and γ, while those obtained from DMSO are the thermodynamically stable Form α at room temperature, as shown in Fig. 2d. In addition, a pure polymorph can still not be obtained by varying the crystallization conditions of PZA in nitrobenzene, shown in Table S3.

3.3. *Influence of mimetic gelator and solvent on PZA polymorphs*

A different pleomorphism of PZA from solution crystallization appeared in the mimetic gel phase crystallization. In order to explore the influence of the mimetic gelator and solvent on PZA polymorphs, a series of control experiments were performed, including non-mimetic gel phase crystallization, solution crystallization with the addition of mimetic gelator and mimetic gel surface crystallization (Tables S4–S6 for experimental details).

As a control, a non-mimetic gelator bearing *n*-propyl substituents was synthesized by a similar procedure as the mimetic gelator as shown in Fig. 3a. The non-mimetic gelator also form gels in nitrobenzene and DMSO and gelation occurs in the presence of PZA (Fig. S1 for non-mimetic gel characterization). However, in the non-mimetic gel phase crystallization, PZA crystals obtained in nitrobenzene proved to be a mixture of Forms β, δ and γ, while in DMSO the non-mimetic gels gave Form α (Fig. 3b), the same polymorphic forms seen in solution crystallization. These observations imply that in mimetic gel phase crystallization the groups of the gelator that have a similar structure to PZA can interact with the PZA molecules to provide specific nucleation sites, changing the polymorphic outcome compared to the solution crystallization results.

The possibility that the mimetic gelator is acting as a solution phase crystallization additive was tested by a further control experiment. The mimetic gelator was dissolved in either nitrobenzene or DMSO at sub-gelation concentration and the resulting solutions used for solution crystallization of PZA. Fig. 3b shows that PZA crystals obtained from nitrobenzene containing dissolved gelator are a mixture of Forms β, δ and γ, while from DMSO Form α was obtained. These outcomes are

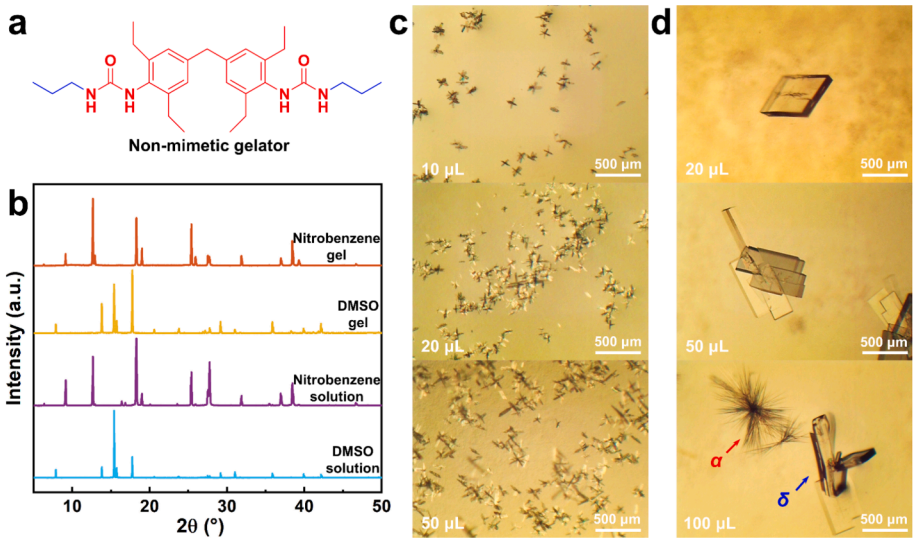

Fig. 3. (a) Chemical structure of non-mimetic gelator; (b) PXRD patterns of PZA obtained from nitrobenzene and DMSO by non-mimetic gel phase crystallization and solution crystallization with the addition of mimetic gelator; (c-d) crystal morphologies of PZA obtained by adding nitrobenzene and DMSO solution on the mimetic gel surface.

consistent with the polymorphism observed from solution crystallization in the pure solvents. Hence only in the gel phase induces the formation of specific polymorphs of PZA implying a role of the array of PYZ mimetic groups on the gel fiber surface. Comparison of the PXRD patterns in Fig. 3b with the reference PXRD patterns of the known PZA forms is shown in Figs. S2 and S3.

In a gel phase crystallization, there are two potential ways for the solvent to influence the polymorphism of PZA, including the role of the gel network structure in indirectly influencing the mass transfer and aggregation of PZA molecules and by solvent effect to directly influence the nucleation behavior of PZA. To clarify the role of solvents, gel surface crystallization was conducted using the mimetic gel in nitrobenzene as a substrate with dropwise addition of supersaturated solutions of PZA in either nitrobenzene or DMSO, respectively. Fig. 3c and 3d show the PZA crystals that formed on the gel surface, with more crystals forming as the volume of PZA solution added increased. For the nitrobenzene solution, the resulting PZA crystals were clusters of small flakes, identified by PXRD as Form β (Fig. S4). For the DMSO solution layered on the mimetic gel in nitrobenzene, PZA plates were first obtained, while mixed plates and needles were observed when the addition volume increased to 100 μL. The plate crystals were identified as Form δ and needle crystals as Form α (Fig. S5). The crystallization process in the presence of the larger 100 μL volume of PZA-DMSO solution was observed by microscopy, which showed that the Form δ plate crystals first appeared on the gel surface and then the Form α needle crystals appeared in the solution phase (as in conventional solution phase crystallization in DMSO) and subsequently dropped on to the gel surface, indicating the preferential selectivity of mimetic gel surface for Form δ in DMSO solution. Therefore, at the DMSO solution-nitrobenzene gel interface the gel surface crystallization outcome is consistent with the bulk gel phase crystallization and selectively induces crystallization of Form δ. This contrasts to the formation of Form β from the nitrobenzene layering experiment and implies that nitrobenzene and DMSO directly influence the polymorph outcomes through a solvent effect in mimetic gel phase crystallization.

3.4. Polymorphic transformation in mixed solvents

The possible solvent induced polymorphic transformation of PZA was assessed in nitrobenzene-DMSO mixed solvent. The solubility of PZA and the CGC of the mimetic gel were determined at room temperature in binary solvents with different ratios of nitrobenzene and DMSO (Table S7), and solution and mimetic gel phase crystallization were performed under the same conditions at a PZA supersaturation degree of 1.5 (Table S8 for experimental details). Table 1 shows that as the ratio of DMSO in mixed solvents increases, a polymorphic transformation of PZA occurs in both crystallization methods, with polymorph outcomes identified by PXRD (Figs. S6 and S7). For solution crystallization, the PZA crystals transformed from a mixture of Forms β, δ and γ to Form α as the DMSO content was increased from 25 % to 50 %. However, for gel phase crystallization, the PZA crystals changed from Forms β to a mixture of Forms β and δ then ultimately to pure Form δ as the DMSO content increased from 0.5 % to 5 %. The polymorphic transformation of PZA in gel phase crystallization initiated at much lower DMSO content and only two polymorphs appeared in all ratios of binary solvent. This implies a synergistic interaction of the mimetic gelator and solvent on the selective crystallization of PZA polymorphs.

3.5. Impact of gel and solvent on the nucleation behavior of PZA

To explain the templating effect and interaction mode of the mimetic gelator and solvent on PZA polymorphism in gel phase crystallization, FTIR spectroscopy was used to characterize the intermolecular interaction of PZA during nucleation. Fig. 4a shows the FTIR spectra of nitrobenzene and DMSO gels containing PZA. Although most of the absorption peaks are caused by the solvents, the peaks relating to the carbonyl group (C═O) around 1700 cm^{-1} are significantly different between both gels. The FTIR of the mimetic gels without PZA and PZA solutions were further tested, showing that the difference in the C═O

Table 1
PZA crystals obtained by solution and mimetic gel phase crystallization in nitrobenzene-DMSO solvents.

Content of DMSO (%)	Form	
	Solution	Gel phase
0	$\beta+\delta+\gamma$	β
0.5	$\beta+\delta+\gamma$	β
1	$\beta+\delta+\gamma$	$\beta+\delta$
3	$\beta+\delta+\gamma$	$\beta+\delta$
5	$\beta+\delta+\gamma$	δ
10	$\beta+\delta+\gamma$	δ
25	$\beta+\delta+\gamma$	δ
50	α	δ
75	α	δ
100	α	δ

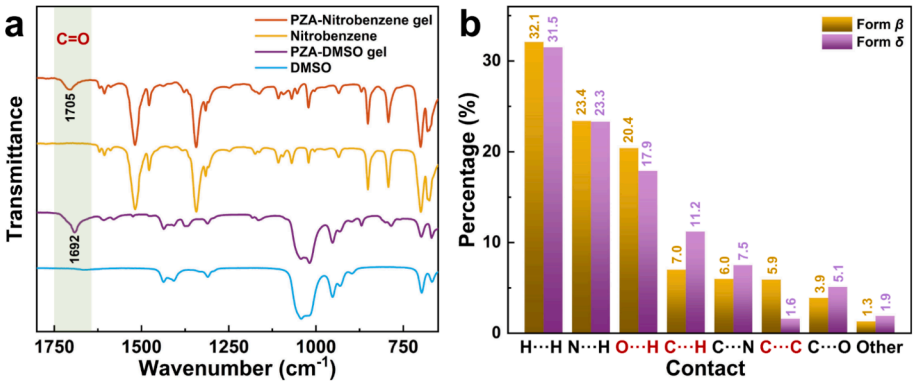

Fig. 4. (a) FTIR spectra of PZA-containing nitrobenzene and DMSO gels and pure solvents; (b) contribution of different contacts to packing structure of Forms β and δ.

position in both gels is only related to the PZA intermolecular interactions (Figs. S8 and S9). Compared to the nitrobenzene gel, the C═O peak of PZA in the DMSO gel is shifted from 1705 to 1692 cm^{-1} with a slight change in peak shape.

There is only one oxygen atom and one carbonyl group in the PZA molecule (Fig. 1a), so it can be considered that in the packing structure of the crystals, the oxygen atom of the C═O can act as a hydrogen bonding acceptor, and the carbon atom of the C═O neighboring the pyrazine group can be involved in the aromatic stacking interaction, as demonstrated by Hirshfeld surface analysis of PZA polymorphs (Fig. S10). The contribution of different contacts to the packing structure was calculated for Forms β and δ, corresponding to the PZA polymorphs obtained in nitrobenzene and DMSO mimetic gel phase crystallization, as shown in Fig. 4b. The H…H and N…H contacts in both polymorphs contribute the highest percentage without significant difference, whereas the main differences in packing modes between Forms β and δ are O···H, C···H and C···C contacts, which differ by 2.5 %, 4.2 % and 4.3 %, respectively. The O···H contact reflects the formation of hydrogen bonding, and the C···H and C···C contacts are associated with aromatic stacking interactions, with all three contacts involving oxygen and carbon atoms in the C═O of PZA molecule. Therefore, it is possible that the mimetic gelator and solvent in the gel phase crystallization influence the nucleation behavior by close interaction with the C═O of PZA molecule to induce PZA polymorphs of Forms β and δ.

4. Conclusion

The supramolecular gels with a specifically targeted gelator that mimics the molecular structure of the highly polymorphic substrate PZA selectively induce the crystallization of metastable polymorphs of Forms β and δ in nitrobenzene and DMSO, respectively. Under the same conditions, crystallization from solution, non-mimetic gel phase and solutions containing dissolved mimetic gelator all give mixtures of Forms β, δ and γ or stable Form α in nitrobenzene and DMSO, respectively, illustrating the special advantage of mimetic gel phase crystallization in obtaining the pure metastable Form β of PZA. Mimetic gel surface crystallization shows similar polymorphic results to gel phase crystallization and further combines with gel phase crystallization in mixed solvents, suggesting that the template effect of mimetic gelator and the solvent-mediated effect synergistically induce the PZA polymorphism. Despite the difficulty in elucidating the process of gel phase crystallization, the combination of analyzing the intermolecular interactions of PZA in nucleation and the packing modes of PZA polymorphs confirmed that the mimetic gelator and solvent can selectively crystalize Forms β and δ mainly through close interactions with the carbonyl group of PZA.

The obtained metastable polymorphs of Forms β and δ have significant advantages in solubility and bioavailability, especially this is the first time to obtain pure Forms β at room temperature, which is essential for quality control and formulation development of PZA. This study also proves that the supramolecular gel designed by drug molecule structure can influence the pharmaceutical polymorphism in a targeted way, providing insight into the interaction modes in gel phase crystallization. However, the crystal growth mechanism and the link between the nucleus ordering and final crystal structure are not well understood and will be the subject of future work.

CRediT authorship contribution statement

Qi Zhang: Writing – original draft, Formal analysis, Conceptualization. **Yizhen Yan:** Formal analysis. **Yisheng Xu:** Investigation, Formal analysis. **Xiangyang Zhang:** Supervision, Conceptualization. **Jonathan W. Steed:** Writing – review & editing, Supervision, Resources, Project administration, Conceptualization.

Declaration of competing interest

The authors declare that they have no known competing financial interests or personal relationships that could have appeared to influence the work reported in this paper.

Acknowledgements

YishengXu thanks for the support of National Key Research and Development Program of the International Scientific and Technological Innovation Cooperation Project among Governments (2021YFE0100400). Qi Zhang thanks the financial support from the China Scholarship Council (202306740019). Xiangyang Zhang acknowledges the support of the National Natural Science Foundation of China (NSFC, No. 22078093) and Natural Science Foundation of Shanghai Municipality (No. 23ZR1417100).

Appendix A. Supplementary data

Supplementary data gel screening, characterization of non-mimetic gel, crystallization experiment details, crystallization in mixed solvent, FTIR spectra and Hirshfeld surface analysis. This material is available from the Elsevier or the author. Supplementary data to this article can be found online at https://doi.org/10.1016/j.jcis.2025.02.093.

Data availability

Underlying data for this work comprising PXRD, FTIR and NMR data can be obtained from doi: 10.15128/r1df65v7911.

References

[1] L.S. Taylor, D.E. Braun, L. Tajber, J.W. Steed, Crystallizing the role of solid-state form in drug delivery, Cryst. Growth Des. 22 (8) (2022) 4663–4665, https://doi.org/10.1021/acs.cgd.2c00760.

[2] Z. Gao, S. Rohani, J. Gong, J. Wang, Recent developments in the crystallization process: toward the pharmaceutical industry, Engineering 3 (3) (2017) 343–353, https://doi.org/10.1016/J.ENG.2017.03.022.

[3] J.W. Steed, 21st century developments in the understanding and control of molecular solids, Chem. Commun. 54 (94) (2018) 13175–13182, https://doi.org/10.1039/C8CC08277D.

[4] D. Singhal, W. Curatolo, Drug polymorphism and dosage form design: a practical perspective, Adv. Drug Deliver. Rev. 56 (3) (2004) 335–347, https://doi.org/10.1016/j.addr.2003.10.008.

[5] R. Contreras-Montoya, L.Á. de Cienfuegos, J.A. Gavira, J.W. Steed, Supramolecular gels: a versatile crystallization toolbox, Chem. Soc. Rev. 53 (21) (2024) 10604–10619, https://doi.org/10.1039/D4CS00271G.

[6] H. Sharma, B.K. Kalita, D. Pathak, B. Sarma, Low molecular weight supramolecular gels as a crystallization matrix, Cryst. Growth Des. 24 (1) (2023) 17–37, https://doi.org/10.1021/acs.cgd.3c01211.

[7] A.J. Savyasachi, O. Kotova, S. Shanmugaraju, S.J. Bradberry, G.M. Ó'Máille, T. Gunnlaugsson, Supramolecular chemistry: a toolkit for soft functional materials and organic particles, Chem 3 (5) (2017) 764–811, https://doi.org/10.1016/j.chempr.2017.10.006.

[8] Y. Diao, K.E. Whaley, M.E. Helgeson, M.A. Woldeyes, P.S. Doyle, A.S. Myerson, T. A. Hatton, B.L. Trout, Gel-induced selective crystallization of polymorphs, J. Am. Chem. Soc. 134 (1) (2012) 673–684, https://doi.org/10.1021/ja210006t.

[9] H.B. Eral, M. O'Mahony, R. Shaw, B.L. Trout, A.S. Myerson, P.S. Doyle, Composite hydrogels laden with crystalline active pharmaceutical ingredients of controlled size and loading, Chem. Mater. 26 (21) (2014) 6213–6220, https://doi.org/10.1021/cm502834h.

[10] M.A. Rahim, Y. Hata, M. Björnmalm, Y. Ju, F. Caruso, Supramolecular metal–phenolic gels for the crystallization of active pharmaceutical ingredients, Small 14 (26) (2018) 1801202, https://doi.org/10.1002/smll.201801202.

[11] J.A. Foster, M.-O.-M. Piepenbrock, G.O. Lloyd, N. Clarke, J.A. Howard, J.W. Steed, Anion-switchable supramolecular gels for controlling pharmaceutical crystal growth, Nat. Chem. 2 (12) (2010) 1037–1043, https://doi.org/10.1038/nchem.859.

[12] S.S. Jayabhavan, J.W. Steed, K.K. Damodaran, Crystal habit modification of metronidazole by supramolecular gels with complementary functionality, Cryst. Growth Des. 21 (9) (2021) 5383–5393, https://doi.org/10.1021/acs.cgd.1c00659.

[13] S.R. Kennedy, C.D. Jones, D.S. Yufit, C.E. Nicholson, S.J. Cooper, J.W. Steed, Tailored supramolecular gel and microemulsion crystallization strategies–is isoniazid really monomorphic? CrstEngComm 20 (10) (2018) 1390–1398, https://doi.org/10.1039/C8CE00066B.

[14] C.R. Taylor, M.T. Mulvee, D.S. Perenyi, M.R. Probert, G.M. Day, J.W. Steed, Minimizing polymorphic risk through cooperative computational and experimental exploration, J. Am. Chem. Soc. 142 (39) (2020) 16668–16680, https://doi.org/10.1021/jacs.0c06749.

[15] J.A. Foster, K.K. Damodaran, A. Maurin, G.M. Day, H.P. Thompson, G.J. Cameron, J.C. Bernal, J.W. Steed, Pharmaceutical polymorph control in a drug-mimetic supramolecular gel, Chem. Sci. 8 (1) (2017) 78, https://doi.org/10.1039/C6SC04126D.

[16] L. Kaufmann, S.R. Kennedy, C.D. Jones, J.W. Steed, Cavity-containing supramolecular gels as a crystallization tool for hydrophobic pharmaceuticals, Chem. Commun. 52 (66) (2016) 10113–10116, https://doi.org/10.1039/C6CC04037C.

[17] I. Torres-Moya, A. Sánchez, B. Saikia, D.S. Yufit, P. Prieto, J.R. Carrillo, J.W. Steed, Highly thermally resistant bisamide gelators as pharmaceutical crystallization media, Gels 9 (1) (2022) 26, https://doi.org/10.3390/gels9010026.

[18] B. Saikia, M.T. Mulvee, I. Torres-Moya, B. Sarma, J.W. Steed, Drug mimetic organogelators for the control of concomitant crystallization of barbital and thalidomide, Cryst. Growth Des. 20 (12) (2020) 7989–7996, https://doi.org/10.1021/acs.cgd.0c01240.

[19] D.K. Kumar, J.W. Steed, Supramolecular gel phase crystallization: orthogonal self-assembly under non-equilibrium conditions, Chem. Soc. Rev. 43 (7) (2014) 2080–2088, https://doi.org/10.1039/C3CS60224A.

[20] A. Dawn, K.S. Andrew, D.S. Yufit, Y. Hong, J.P. Reddy, C.D. Jones, J.A. Aguilar, J. W. Steed, Supramolecular gel control of cisplatin crystallization: Identification of a new solvate form using a cisplatin-mimetic gelator, Cryst. Growth Des. 15 (9) (2015) 4591–4599, https://doi.org/10.1021/acs.cgd.5b00840.

[21] J.L. Andrews, S.R. Kennedy, D.S. Yufit, J.F. McCabe, J.W. Steed, Designer gelators for the crystallization of a salt active pharmaceutical ingredient— Mexiletine hydrochloride, Cryst. Growth Des. 22 (11) (2022) 6775–6785, https://doi.org/10.1021/acs.cgd.2c00925.

[22] Y. Zhang, D. Mitchison, The curious characteristics of pyrazinamide: a review, Int. J. Tuberc. Lung d. 7 (1) (2003) 6–21.

[23] D. Maher, P. Chaulet, S. Spinaci, A. Harries, Treatment of tuberculosis: guidelines for national programmes 2 (1997) 1–77.

[24] S. Cherukuvada, R. Thakuria, A. Nangia, Pyrazinamide polymorphs: relative stability and vibrational spectroscopy, Cryst. Growth Des. 10 (9) (2010) 3931–3941, https://doi.org/10.1021/cg1004424.

[25] G. Rajalakshmi, V.R. Hathwar, P. Kumaradhas, Crystal Engineering, Materials, Intermolecular interactions, charge-density distribution and the electrostatic properties of pyrazinamide anti-TB drug molecule: an experimental and theoretical charge-density study, Acta Crystallogr. B 70 (3) (2014) 568–579, https://doi.org/10.1107/S205252061303388X.

[26] K.N. Jarzembska, A.A. Hoser, R. Kamiński, A.Ø. Madsen, K. Durka, K. Wozniak, Combined experimental and computational studies of pyrazinamide and nicotinamide in the context of crystal engineering and thermodynamics, Cryst. Growth Des. 14 (7) (2014) 3453–3465, https://doi.org/10.1021/cg500376z.

[27] N. Wahlberg, P. Ciochon, V. Petricek, A.Ø. Madsen, Polymorph stability prediction: on the importance of accurate structures: a case study of pyrazinamide, Cryst. Growth Des. 14 (1) (2014) 381–388, https://doi.org/10.1021/cg400800u.

[28] K. Li, G. Gbabode, M. Sanselme, B. Nicolaï, N. Guiblin, I.B. Rietveld, Relation between twinning and disorder in the γ form of pyrazinamide, Cryst. Growth Des. 23 (4) (2023) 2463–2469, https://doi.org/10.1021/acs.cgd.2c01419.

[29] A.A. Hoser, T. Rekis, A.Ø. Madsen, Crystal engineering, materials, dynamics and disorder: on the stability of pyrazinamide polymorphs, Acta Crystallogr. B 78 (3) (2022) 416–424, https://doi.org/10.1107/S2052520622004577.

[30] A. Maharana, D. Sarkar, Solubility measurements and thermodynamic modeling of pyrazinamide in five different solvent-antisolvent mixtures, Fluid Phase Equilibr. 497 (2019) 33–54, https://doi.org/10.1016/j.fluid.2019.06.004.

[31] J. Zhang, Z. Liang, S. Ji, X. Wang, P. Lan, The thermal behavior of pyrazinamide in 12 solvents from 288.15 to 328.15 k, J. Mol. Liq. 329 (2021) 115572, https://doi.org/10.1016/j.molliq.2021.115572.

[32] Y. Luo, Q. Liu, L. Yang, W. Wang, Y. Ling, B. Sun, Quantitative comparisons between α, β, γ, and δ pyrazinamide (PZA) polymorphs, Res. Chem. Intermediat. 41 (2015) 7059–7072, https://doi.org/10.1007/s11164-014-1798-z.

[33] R.A. Castro, T.M. Maria, A.O. Évora, J.C. Feiteira, M.R. Silva, A.M. Beja, J. Canotilho, M.E.S. Eusébio, A new insight into pyrazinamide polymorphic forms and their thermodynamic relationships, Cryst. Growth Des. 10 (1) (2010) 274–282, https://doi.org/10.1021/cg900890n.

[34] K. Zhang, S. Xu, S. Liu, W. Tang, X. Fu, J. Gong, Novel strategy to control polymorph nucleation of gamma pyrazinamide by preferred intermolecular interactions during heterogeneous nucleation, Cryst. Growth Des. 18 (9) (2018) 4874–4879, https://doi.org/10.1021/acs.cgd.8b00943.

[35] G. Baaklini, V. Dupray, G. Coquerel, Inhibition of the spontaneous polymorphic transition of pyrazinamide γ form at room temperature by co-spray drying with 1, 3-dimethylurea, Int. J. Pharmaceut. 479 (1) (2015) 163–170, https://doi.org/10.1016/j.ijpharm.2014.12.063.

[36] Y. Song, Y. Wu, Y. Jiang, H. Yang, Y. Jiang, Polymers and solvent-induced polymorphic selection and preferential orientation of pyrazinamide crystal, Cryst. Growth Des. 20 (1) (2019) 352–361, https://doi.org/10.1021/acs.cgd.9b01287.

[37] W. Liu, Z. Li, Z. Wang, Z. Huang, C. Sun, S. Liu, Y. Jiang, H. Yang, Interfaces, Functional system based on glycyrrhizic acid supramolecular hydrogel: toward polymorph control, stabilization, and controlled release, ACS Appl. Mater. Inter. 15 (6) (2023) 7767–7776, https://doi.org/10.1021/acsami.2c19903.

[38] K. Zhang, S. Xu, J. Gong, W. Tang, Revealing the critical role of template functional group ordering in the template-directed crystallization of pyrazinamide, CrstEngComm 21 (42) (2019) 6382–6389, https://doi.org/10.1039/C9CE01236B.

[39] Y. Takaki, Y. Sasada, T. Watanabé, The crystal structure of α-pyrazinamide, Acta Crystallogr. 13 (9) (1960) 693–702, https://doi.org/10.1107/S0365110X60001680.

[40] G. Rø, H. Sørum, The crystal and molecular structure of β-pyrazinecarboxamide, Acta Crystallogr. B 28 (4) (1972) 991–998, https://doi.org/10.1107/S0567740872003589.

[41] G. Rø, H. Sørum, The crystal and molecular structure of δ-pyrazinecarboxamide, Acta Crystallogr. B 28 (6) (1972) 1677–1684, https://doi.org/10.1107/S0567740872004856.

[42] P.R. Spackman, M.J. Turner, J.J. McKinnon, S.K. Wolff, D.J. Grimwood, D. Jayatilaka, M.A. Spackman, CrystalExplorer: a program for Hirshfeld surface analysis, visualization and quantitative analysis of molecular crystals, J. Appl. Crystallogr. 54 (3) (2021) 1006–1011, https://doi.org/10.1107/S1600576721002910.

[43] C.D. Jones, S.R. Kennedy, M. Walker, D.S. Yufit, J.W. Steed, Scrolling of supramolecular lamellae in the hierarchical self-assembly of fibrous gels, Chem 3 (4) (2017) 603–628, https://doi.org/10.1016/j.chempr.2017.09.001.

[44] C.D. Jones, L.J. Kershaw Cook, A.G. Slater, D.S. Yufit, J.W. Steed, Scrolling in supramolecular gels: a designer's guide, Chem. Mater. 36(6) (2024) 2799–2809, Doi: 10.1021/acs.chemmater.3c03013.

[45] A. Dawn, M. Mirzamani, C.D. Jones, D.S. Yufit, S. Qian, J.W. Steed, H. Kumari, Investigating the effect of supramolecular gel phase crystallization on gel nucleation, Soft Matter 14 (46) (2018) 9489–9497, https://doi.org/10.1039/C8SM01916A.